Distannylated Isothianaphthene: A Versatile Building Block for Low Bandgap Conjugated Polymers

Yang Qin,[†] Jung Yong Kim,[‡] C. Daniel Frisbie,*[,‡] and Marc A. Hillmyer*[,†]

Department of Chemistry, University of Minnesota, 207 Pleasant St. SE, Minneapolis, Minnesota 55455-0431, and Department of Chemical Engineering & Materials Science, University of Minnesota, 421 Washington Ave. SE, Minneapolis, Minnesota 55455-0431

Received May 23, 2008

ABSTRACT: A novel 1,3-distannylated isothianaphthene (**1**) was synthesized in high yield by dilithiation of isothianaphthene (ITN) followed by treatment with trimethyltin chloride. Compound **1** is stable in the absence of oxygen and was fully characterized by multinuclear NMR spectroscopy, mass spectrometry, and elemental analysis. We used **1** as a building block for the synthesis of a series of conjugated polymers with alternating structures through Stille-type coupling reactions with dibromo and diiodo compounds. The resulting polymers were characterized by size exclusion chromatography, multinuclear NMR spectroscopy, mass spectrometry, and differential scanning calorimetry. The HOMO−LUMO energy bandgaps of these materials, estimated from UV−vis spectroscopy and cyclic voltammetry (CV), ranged from 1.66 to 2.56 eV depending on the chemical nature of the dihalogenated units. Bulk heterojunction photovoltaic (PV) devices constructed using blends of the ITN-containing copolymers and [6,6]-phenyl-C_{61}-butyric acid methyl ester (PCBM) gave power conversion efficiencies ranging from 0.12% to 0.43%.

Introduction

Soluble conjugated polymers possessing small HOMO−LUMO energy bandgaps have been the subject of extensive research in the field of organic photovoltaic (OPV) devices.[1−3] Low bandgap conjugated polymers typically absorb in the red and near-IR region and better match the solar photon flux spectrum. This overlap with the solar spectrum has been thought to be one of the key factors needed for improving OPV device performance through increases in the short-circuit current (J_{SC}).[4] These polymers can be designed to have optimal positioning of the HOMO/LUMO energy levels relative to electron acceptors such as the commonly encountered fullerene derivatives in bulk heterojunction (BHJ) devices.[5−7] Low bandgap conjugated polymers can also be designed to be soluble in a wide range of organic solvents allowing for favorable solution processability, such as in ink-jet printing and roll-to-roll processes, a prerequisite for low-cost manufacturing and ultimate commercialization of OPV devices.[8,9]

One intriguing example of a low bandgap conjugated polymer is poly(isothianaphthene) (PITN), introduced by Wudl et al. in 1984 through either electrochemical polymerization or chemical oxidation methods.[10] Although the bandgap of PITN has been determined both optically and electrochemically to be 1.0−1.2 eV,[11,12] one of the lowest known to date, this dark-blue material is insoluble in typical organic solvents and thus unsuitable for common OPV device fabrication techniques. As a result, PITNs with various side chains as solubilizing groups, including alkyl,[13−15] alkoxy,[16,17] and thioalkyl[17] functionalities, have been proposed and synthesized. However, these polymers have rarely been applied in OPV devices presumably due to their poor processability and film-forming ability. One of the few examples was shown by Goris et al.[18] An OPV device, constructed using blends containing 1:1 (w/w) poly(5,6-dithiooctylisothianaphthene): PCBM as the active layer, gave an open-circuit voltage (V_{OC}) of 0.2 V and a J_{SC} of 0.04 mA/cm^2 under simulated AM 1.5 illumination.

Another common synthetic strategy is to incorporate isothianaphthene (ITN) units into copolymer structures in an alternating fashion to form a so-called donor−acceptor arrangement, which is thought to result in lower bandgaps by mixing the HOMO/LUMO levels of individual donor and acceptor monomers.[19−21] The most commonly encountered example involving ITN is poly(1,3-dithienylisothianapthene) (PDTI) and its derivatives. These polymers are typically obtained by electrochemical or chemical oxidative polymerization of 1,3-dithienylisothianapthene monomers commonly synthesized using Lawesson's reagent.[22,23] The photovoltaic behavior of PDTIs was investigated by Shaheen et al.[24] Although the bandgaps of these polymers were determined to be 1.2−1.8 eV depending on the substituents, their low molecular weights significantly limited their film-forming ability. In fact, poly(methyl methacrylate) (PMMA) had to be employed as a host matrix material for casting pinhole-free films. The efficiencies of the resulting OPV devices ranged from 0.04% to 0.4%. Alternatively, ITN-containing copolymers can be obtained through condensation polymerization with difunctionalized monomers. For instance, Saito et al. reported the synthesis of a poly(arylenevinylene)-type copolymer containing ITN units through Wittig reaction between 2,5-bis(dodecyloxy)-*p*-xylylenebis(triphenylphosphonium bromide) and isothianaphthene-1,3-dicarbaldehyde, and the bandgap of the resulting polymer was determined by cyclic voltammetry to be ca. 1.7 eV.[25] The same group also synthesized similar polymers with ITN−vinylene alternating structures through titanium-induced McMurry reaction of an alkoxy-isothianaphthene-1,3-dicarbaldehyde, and the resulting soluble polymer had an extended absorption up to 900 nm in chloroform solution.[26] Furthermore, Kiebooms et al. reported the synthesis of a series of low bandgap ITN-containing copolymers with liquid crystalline side chains through condensation between a disilylated ITN monomer, first synthesized by Okuda et al.,[27] and aldehydes bearing different substituents.[28] These polymers have relatively low molecular weights (M_n = 5000−8000) and optical bandgaps ranging from 1.2 to 1.3 eV.

The ITN-containing polymers described above are typically obtained by reactions specific to the monomers used, and there has not been a general method for the synthesis of ITN-containing copolymers with AB/donor−acceptor type structures.

* Corresponding authors. E-mail: frisbie@cems.umn.edu (C.D.F.); hillmyer@umn.edu (M.A.H.).
[†] Department of Chemistry.
[‡] Department of Chemical Engineering & Materials Science.

10.1021/ma8011575 CCC: $40.75
Published on Web 07/02/2008

Scheme 1. Synthesis of Monomers

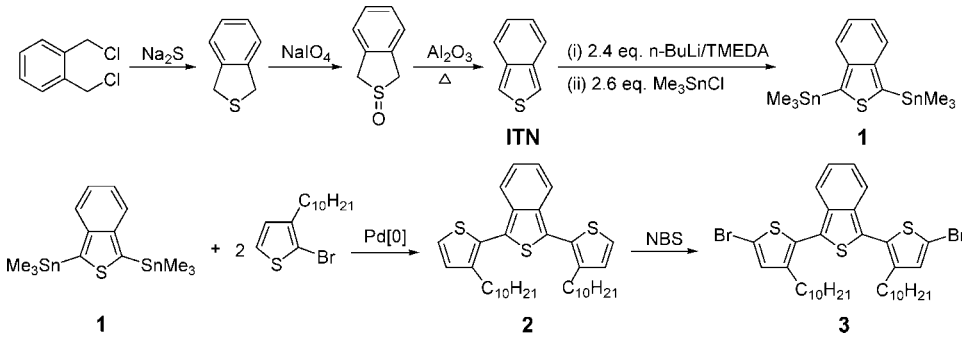

Herein we report the synthesis of a new distannylated ITN monomer **1** that can be used as a versatile building block for a series of ITN-containing copolymers through Pd[0]-catalyzed cross-coupling reactions.[29] Evaluation of OPV devices constructed using the resulting polymers is also presented and discussed.

Results and Discussion

Monomer Synthesis and Characterization. ITN was synthesized in three steps according to the procedure described by Christensen et al. (Scheme 1).[30] The dilithiation of ITN was previously described by Saito et al. to take place with excess *n*-BuLi and tetramethylethylenediamine (TMEDA) in refluxing hexanes for 0.5 h.[25] We found that by switching the solvent to THF the reaction proceeded smoothly to completion in a few hours at room temperature. After addition of Me_3SnCl and aqueous work-up, monomer **1** was isolated in 62% yield as a pale yellow solid through recrystallization from petroleum ether.

Like most ITN compounds, **1** is only moderately stable as it darkens and becomes partially insoluble upon storage in air during a period of 1 week, presumably due to hydrolytic destannylation and oxygen-induced oxidative polymerization. However, **1** is stable under inert atmosphere at low temperature. No detectable decomposition was found by NMR spectroscopy after storage at −20 °C under a N_2 atmosphere for 3 months. Compound **1** was characterized by solution ^1H and ^{13}C NMR spectroscopy (Figure S1). The signal patterns and integration perfectly match the proposed structure. Monomer **1** was further characterized by low-resolution direct probe mass spectrometry (EI mode) and elemental analysis. As seen in the mass spectrum of **1** (Figure 1), the complex isotope pattern is caused mainly by the two Sn atoms that exist naturally as multiple isotopes; the measured pattern and relative intensities closely match those calculated for $C_{14}H_{22}SSn_2$. Thus, monomer **1** was unambiguously identified as the only other stable dimetallic 1,3-disubstituted ITN derivative in the past 30 years.[31]

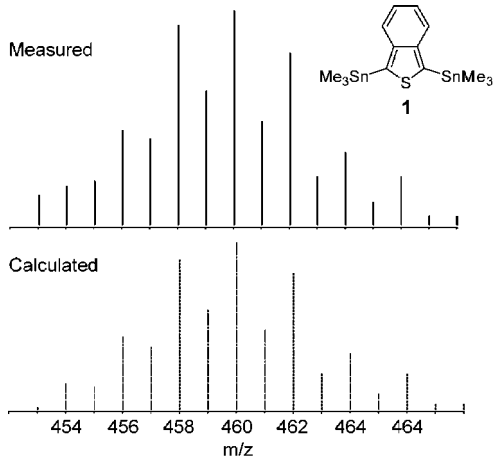

Figure 1. Low-resolution direct probe mass spectrum (electron impact mode) of monomer **1**.

Monomer **1** can be used to access a wide range of ITN-containing monomers and polymers through Stille-type[32,33] coupling reactions. For instance, **1** can react with 2-bromo-3-decylthiophene in the presence of $Pd[PPh_3]_4$ to give **2**, a 1,3-dithienylisothianaphthene (DTI) derivative (Scheme 1). DTIs have previously been synthesized through the methods described by Mohanakrishnan et al.[22] and Vangeneugden et al.,[23] which involve harsh conditions and very reactive species such as PCl_5 as well as Grignard and Lawesson's reagents, and thus have limited compatibility with various functional groups. Our method represents a milder and more efficient route to DTI derivatives, since Stille-type reactions are tolerant to a variety of functionalities. Monomer **2** was further brominated with 2 equiv of *N*-bromosuccinimide (NBS) to give **3** (Scheme 1), which in turn can be used as a coupling partner with **1** for the synthesis of ITN-containing copolymers as discussed below.

Polymer Synthesis and Characterization. Three ITN-containing copolymers, **PITN-*co*-Fl**, **PITN-*co*-3HT**, and **PITN-*co*-3DT** as shown in Scheme 2, were obtained through Stille-type coupling reactions of monomer **1** with stoichiometric amounts of 9,9′-dihexyl-2,7-dibromofluorene, 2,5-diiodo-3-hexylthiophene,[34] and monomer **3**, respectively. The reactions were conducted in degassed anhydrous toluene with 10% $Pd[PPh_3]_4$ at elevated temperatures for 24−72 h (Table 1). Residual catalysts were then removed by passing the reaction mixtures through short columns of silica gel, and the polymers were isolated in 30−70% yield by repeated precipitation into acetone followed by drying under vacuum at room temperature for 12 h.

All three ITN-containing copolymers are soluble in CH_2Cl_2, $CHCl_3$, and aromatic solvents such as benzene, toluene, and *o*-dichlorobenzene. The polymers were characterized by solution ^1H and ^{13}C NMR spectroscopy. Figure 2 shows the ^1H NMR spectra of **PITN-*co*-3HT** in C_6D_6 and **PITN-*co*-3DT** in toluene-d_8.[35] Notably, the chemically equivalent ITN protons 4 and 7 in both polymers give two signals with equal intensities at δ 8.2 and 7.9, one of which is assigned to the protons adjacent to the alkyl groups and the other to the protons away from the alkyl groups. The thiophene protons appear as a single peak at δ 7.4, and the ITN H-5,6 give only one peak at ca. δ 7.0 since they are less influenced by the adjacent alkyl substituents. The signals for **PITN-*co*-3HT** are significantly broader than those for **PITN-*co*-3DT** since the former was synthesized from an asymmetric starting material, 2,5-diiodo-3-hexylthiophene, leading to a regiorandom structure that normally gives broader ^1H NMR signals. Another possible reason is that **PITN-*co*-3HT** has a relatively low molecular weight (Table 1), and thus the end groups should have more effect on the chemical shifts of adjacent units. **PITN-*co*-3DT** was constructed with symmetrical

Scheme 2. Synthesis of ITN-Containing Copolymers

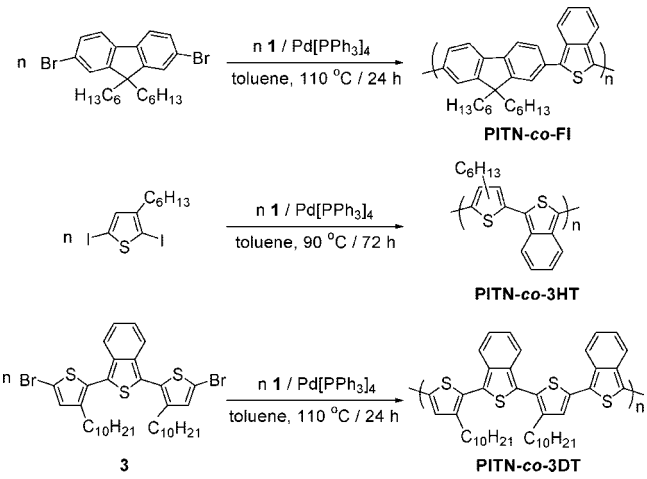

Table 1. ITN-Containing Copolymers

	temp (°C)[a]	time (h)[b]	yield (%)[c]	M_n (kg/mol)[d]	M_w (kg/mol)[d]	PDI[d]	T_g (°C)[e]
PITN-*co*-Fl	110	24	70	3.6	20	5.5	27
PITN-*co*-3HT	90	72	30	5.2	9.1	1.8	65
PITN-*co*-3DT	110	24	51	11	28	2.5	29

[a] Reaction temperature. [b] Reaction time. [c] Isolated yield. [d] SEC refractive index (RI) detector calibrated with polystyrene standards, $CHCl_3$ as eluent (1 mL/min). [e] Glass transition temperature, taken from the onset of the second heating curve, 10 °C/min.

components, leading to regioregular structure. The significantly higher molecular weight of **PITN-*co*-3DT** should also lead to negligible end-group effects. Indeed, sharper signals are observed for **PITN-*co*-3DT**. The ITN-H4,7 signals are well-resolved, indicating similar environment for each of these protons along the entire polymer chain.

Molecular weights of these polymers were determined by size exclusion chromatography (SEC) in $CHCl_3$ against polystyrene standards, and the results are summarized in Table 1. All polymers show monomodal SEC profiles (Figure S3) and exhibit somewhat broad molecular weight distributions. A significant high molecular weight tail is observed for **PITN-*co*-Fl** that likely accounts for the unusually high polydispersity index (PDI). **PITN-*co*-3HT** and **PITN-*co*-3DT** have similar PDI values, but the latter has a significantly higher molecular weight (Table 1). Since both polymers were synthesized under similar conditions and iodine is even a better leaving group than bromine, the lower molecular weight of **PITN-*co*-3HT** is likely caused by the steric hindrance of the 3-hexyl group of 2,5-diiodo-3-hexylthiophene, leading to inefficient coupling of the iodine atom at the 2-position. Such steric hindrance is absent in the synthesis of **PITN-*co*-3DT**. Moreover, the relatively low molecular weights of these polymers could also be caused by undesirable side reactions either with the monomers or at the ends of propagating polymer chains which would eventually lead to stoichiometric imbalance of the monomers as well as oligomers with unreactive "dead ends". Thus, we performed matrix-assisted laser desorption/ionization-time-of-flight (MALDI-TOF) measurements on these ITN-containing copolymers. In the MALDI-TOF spectra of all three polymers (Figures S4−S6), the measured molecular weights agree reasonably well with those obtained from SEC, and the mass differences between major signals correspond to the molecular weight of one repeat unit of each polymer. However, repeating fine structures are observed within each major peak in all spectra, indicating different end groups present for these polymers. Indeed, a close examination of these end-group patterns reveals a few possible side reactions during the synthesis, including homocoupling between ITN units and thiophene units, destannylation, and debromination (Figures S4−S6).

These polymers absorb strongly in the UV−vis region both in solution and as thin films. As seen in Figure 3a, **PITN-*co*-Fl** shows two absorption maxima (λ_{max}) in dilute $CHCl_3$ solution (1.01×10^{-5} M based on repeat units) at 339 nm ($\epsilon = 2.5 \times 10^4$ L mol^{-1} cm^{-1}) and 435 nm ($\epsilon = 2.3 \times 10^3$ L mol^{-1} cm^{-1}); from the absorption edge at 510 nm, the optical bandgap of **PITN-*co*-Fl** in solution is estimated to be 2.44 eV. A significant increase in intensity and a red shift to $\lambda_{max} = 450$ nm of the lower energy absorption band are observed for the thin film of **PITN-*co*-Fl** drop-cast from *o*-dichlorobenzene solution (ca. 5 mg/mL), which is likely due to enhanced interaction between polymer chains in the solid state. From the absorption edge at 530 nm, the optical bandgap of **PITN-*co*-Fl** in the solid state is estimated to be 2.34 eV (Table 2). A broadened absorption band at ca. 300 nm is also observed for the film presumably from residual *o*-dichlorobenzene.

PITN-*co*-3HT and **PITN-*co*-3DT**, show similar absorption properties both in dilute solutions and as thin films. As shown in Figure 3b,c, in dilute $CHCl_3$ solution both polymers have λ_{max} at 513 nm ($\epsilon = 9.6 \times 10^3$ L mol^{-1} cm^{-1} for **PITN-*co*-3HT** and 8.1×10^3 L mol^{-1} cm^{-1} for **PITN-*co*-3DT**) and an absorption edge at 670 nm, from which the optical bandgaps of both polymers in solutions are estimated to be 1.85 eV. A significant red shift is observed in the spectra of the polymer films. **PITN-*co*-3HT** experiences a 20 nm red shift of λ_{max} to 533 nm, and a 35 nm shift to λ_{max} of 548 nm is observed for **PITN-*co*-3DT**. This larger red shift in the absorption spectrum for **PITN-*co*-3DT** is likely due to its regioregularity that leads to a better packing of the polymer chains in solid state and thus stronger interchain interactions. The absorption edges of both polymer films are also extended to ca. 750 nm, which corresponds to an optical bandgap of about 1.66 eV (Table 2).

To further explore the relative HOMO/LUMO energies of these polymers, cyclic voltammetry (CV) measurements were performed on thin films drop-cast from *o*-dichlorobenzene solutions (ca. 5 mg/mL) onto a glassy carbon working electrode (Figures S8−S10), and the results are summarized in Table 2. A pseudoreversible oxidation wave with an onset of $E_{ox/onset} = 0.86$ V and a nonreversible reduction wave with an onset of $E_{red/onset} = -1.70$ V were observed for **PITN-*co*-Fl**. According to the empirical correlations suggested by Brédas et al. and Agrawal et al.,[36,37] the HOMO and LUMO energy levels of **PITN-*co*-Fl** are estimated to be $E_{HOMO} = -0.86 - 4.4 = -5.26$ eV and $E_{LUMO} = 1.70 - 4.4 = -2.70$ eV, from which the bandgap is estimated to be $E_{g/CV} = -2.70 - (-5.26) = 2.56$ eV, slightly higher than that obtained from UV−vis absorption measurement ($E_g = 2.34$ eV). **PITN-*co*-3HT** and **PITN-*co*-3DT** showed similar electrochemical responses. Pseudoreversible oxidation waves were observed for both polymers, and no reduction took place up to −2 V, beyond which decomposition of the supporting electrolyte occurred. Similar to the calculation for **PITN-*co*-Fl**, the HOMO energy levels for **PITN-*co*-3HT** and **PITN-*co*-3DT** are estimated from the oxidation onsets to be −5.22 and −5.07 eV, respectively. Since no reduction was observed for both polymers, the LUMO energy levels could only be estimated from the HOMO energy levels and the optical bandgaps to be −3.56 eV for **PITN-*co*-3HT** and −3.41 eV for **PITN-*co*-3DT** (Table 2).

Photovoltaic Devices. PV devices were fabricated with the ITO/PEDOT:PSS/ITN-containing copolymer:PCBM/Al (Figure 5b, inset) bulk heterojunction configuration. We first studied the composition effect of the **PITN-*co*-3DT**:PCBM blend PV devices. **PITN-*co*-3DT** was chosen since it exhibited an attractive combination of low bandgap and good processability among the three polymers. Figure 4a shows the normalized

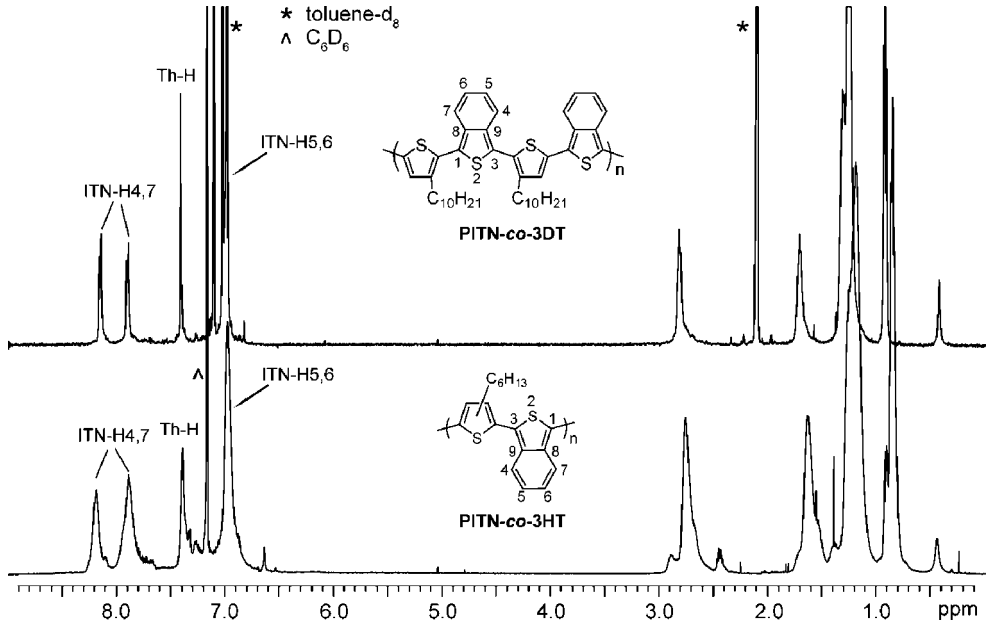

Figure 2. ^{1}H NMR spectra of **PITN-*co*-3HT** (C_6D_6) and **PITN-*co*-3DT** (toluene-d_8).

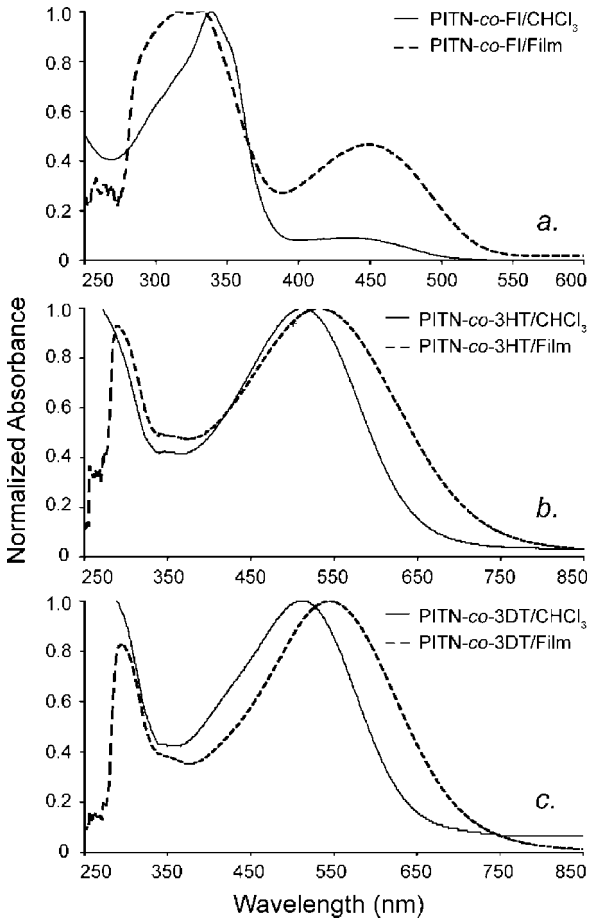

Figure 3. UV−vis absorption spectra of **PITN-*co*-FI** (a), **PITN-*co*-3HT** (b), and **PITN-*co*-3DT** (c) in $CHCl_3$ (1.01×10^{-5}, 2.24×10^{-5}, and 1.68×10^{-5} M based on repeat units, respectively; solid lines) and as thin films drop-cast from *o*-dichlorobenzene solutions (ca. 5 mg/mL) onto ITO-coated glass substrates and dried in air at room temperature (dashed lines). Absorption scales are normalized for clarity.

UV−vis absorption spectra of the **PITN-*co*-3DT**:PCBM blend PV devices (without Al top contact) as a function of composition. While the films of 1:1, 1:2, and 1:3 compositions show similar absorption to that of the pristine polymer film (Figure 3c), a significant blue shift of the absorption onset to ca. 700 nm is observed for the film of 1:4 composition. This blue shift in absorption is likely caused by blending of PCBM molecules with polymer that leads to reduced intermolecular interactions. The device performance was examined under illumination with monochromatic light or 100 mW/cm^2 simulated AM 1.5 irradiation. Figure 4b depicts photocurrent action spectra for the **PITN-*co*-3DT**:PCBM PV devices under monochromatic illumination. The external quantum efficiency or incident photon to current efficiency, IPCE (%), is displayed as a function of wavelength. Maximum quantum efficiency at the absorption apex increases gradually with increasing PCBM content and reaches 20% at 350 nm in the device with 1:4 **PITN-*co*-3DT**:PCBM composition. A significant increase of IPCE (%) between wavelengths of 400 and 500 nm is also observed in this device. Current−voltage characteristics as a function of composition for **PITN-*co*-3DT**:PCBM blend PV devices in dark and under 100 mW/cm^2 simulated AM 1.5 illumination are shown in Figure 4c. No significant current was observed for all devices in the dark at negative bias, and only the dark current for device of 1:4 composition is shown for clarity. However, increase in current at negative bias under illumination was observed in all cases. We believe this is due to an increased collection of generated carriers in a stronger field. By increasing the PCBM content, the maximum power conversion efficiency increases from 0.05% ($V_{OC} = 0.5$ V, $J_{SC} = 0.35$ mA/cm^2, $FF = 29\%$) at 1:1 composition to 0.24% ($V_{OC} = 0.5$ V, $J_{SC} = 1.35$ mA/cm^2, $FF = 35\%$) at 1:4 composition; this trend is similar to that of

Table 2. UV−Vis Absorption and Cyclic Voltammetry Measurements for Thin Films of the ITN-Containing Copolymers

	λ_{edge} (nm)[a]	E_g (eV)[b]	$E_{ox/onset}$ (V)[c]	E_{HOMO} (eV)[d]	$E_{red/onset}$ (V)[e]	E_{LUMO} (eV)
PITN-*co*-FI	530	2.34	0.86	−5.26	−1.70	−2.70[f]
PITN-*co*-3HT	750	1.66	0.82	−5.22		−3.56[g]
PITN-*co*-3DT	750	1.66	0.67	−5.07		−3.41[g]

[a] Absorption edge of polymer film. [b] Optical bandgap estimated from the absorption edge. [c] Onset of oxidation from cyclic voltammogram of polymer film. [d] Estimated from $E_{ox/onset}$. [e] Onset of reduction from cyclic voltammogram of polymer film. [f] Estimated from $E_{red/onset}$. [g] Estimated from E_{HOMO} and optical bandgap E_g.

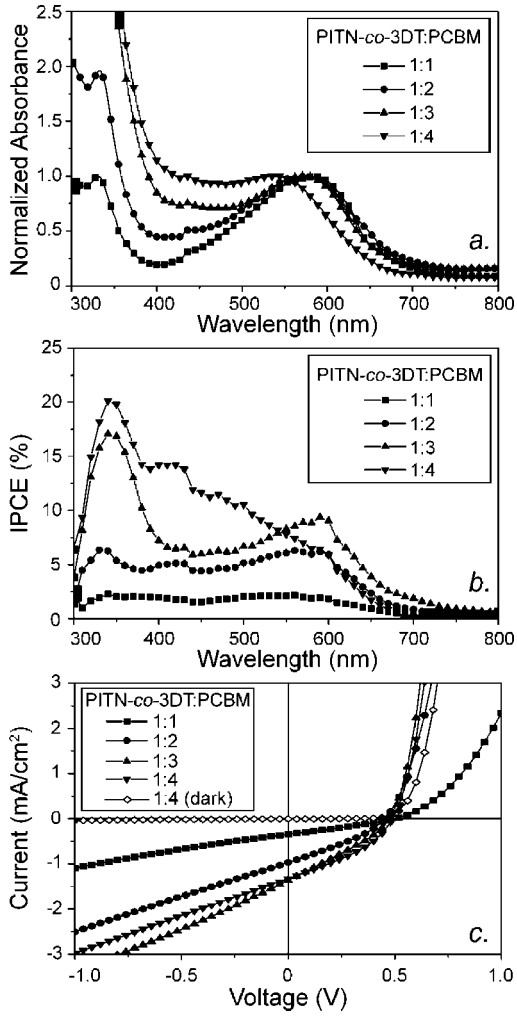

Figure 4. (a) UV−vis absorption spectra as a function of composition for **PITN-*co*-3DT**:PCBM blend PV devices (without Al top contact). (b) Photocurrent action spectra as a function of composition for **PITN-*co*-3DT**:PCBM blend PV devices under illumination with monochromatic light. (c) Current−voltage characteristics as a function of composition for **PITN-*co*-3DT**:PCBM blend PV devices in dark (1:4 composition shown) and under 100 mW/cm^2 simulated AM 1.5 illumination.

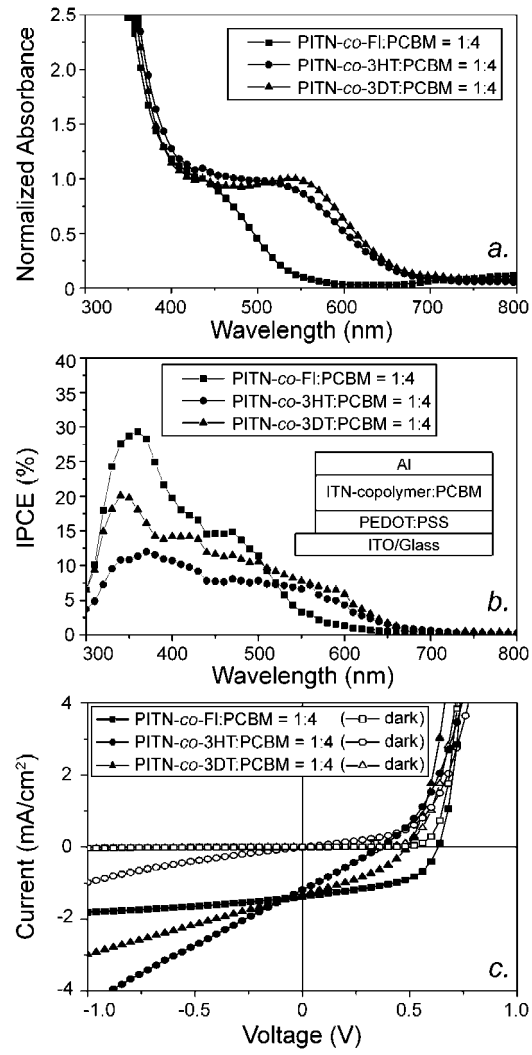

Figure 5. (a) UV−vis absorption spectra of PV devices (without Al top contact) based on ITN-containing copolymer:PCBM blends (1:4 w/w). (b) Photocurrent action spectra of PV devices based on ITN-containing copolymer:PCBM blends (1:4 w/w) under illumination with monochromatic light. Inset: representative device configuration. (c) Current−voltage characteristics for PV devices of the ITN-containing copolymer:PCBM (1:4 w/w) in dark and under 100 mW/cm^2 simulated AM 1.5 illumination.

the performance of the amorphous PPV (poly(*p*-phenylenevinylene)) derivative:fullerene PV devices.[38]

On the basis of the performance of the **PITN-*co*-3DT**:PCBM blend PV devices, we fabricated PV devices for **PITN-*co*-Fl** and **PITN-*co*-3HT** of the same device configuration using the same 1:4 polymer:PCBM composition. In the UV−vis absorption spectra of the PV devices (without Al top contact, Figure 5a), the wider bandgap **PITN-*co*-Fl**:PCBM blend shows an onset of ca. 560 nm relative to the absorption onset at 530 nm in a pure **PITN-*co*-Fl** film. This longer wavelength onset is likely due to PCBM absorption, since a pristine PCBM film shows an absorption edge at 588 nm with a band tail reaching to 650 nm. The **PITN-*co*-3HT**:PCBM blend shows similar absorption behavior to that of the **PITN-*co*-3DT**:PCBM blend with a blue-shifted onset to ca. 700 nm. Maximum quantum efficiencies at the absorption apex are calculated to be 29% for **PITN-*co*-Fl** at 360 nm and 12% for **PITN-*co*-3HT** at 370 nm, compared to 20% for **PITN-*co*-3DT** at 350 nm (Figure 5b). Figure 5c reveals the current−voltage characteristics for the three PV devices in the dark and under 100 mW/cm^2 simulated AM 1.5 illumination, and the results are summarized in Table 3. Although **PITN-*co*-Fl** has the highest bandgap of the three polymers tested, it surprisingly outperforms the other two lower bandgap polymers in PV devices under the same testing conditions. As seen in Figure 5c, no dark current and only a slight increase in current under illumination at negative bias are observed. This is possibly due to the better film-forming property of **PITN-*co*-Fl** despite the lower molecular weight. The effect is more evident in the comparison between the devices made from **PITN-*co*-3HT** and **PITN-*co*-3DT**. Both polymers have similar chemical structures and electronic properties, except that **PITN-*co*-3DT** has longer side chains and 2 times larger molecular weight and thus better processability. Indeed, a dark leakage current at negative bias is observed for the device of **PITN-*co*-3HT** presumably due to its poor film-forming ability, and the PV device of **PITN-*co*-3DT** performs

Table 3. Open-Circuit Voltage (V_{OC}), Short-Circuit Current (J_{SC}), Fill Factor (*FF*), and Power Conversion Efficiency (η) for ITN-Containing Copolymer:PCBM PV Devices

1:4 wt ratio	V_{OC} (V)	J_{SC} (mA/cm^2)	*FF* (%)	η (%)
PITN-*co*-Fl:PCBM	0.63	1.37	50	0.43
PITN-*co*-3HT:PCBM	0.38	1.18	26	0.12
PITN-*co*-3DT:PCBM	0.50	1.35	35	0.24

much better than that of **PITN-*co*-3HT** with significantly higher V_{OC}, J_{SC}, and FF.[39]

Conclusion

We have synthesized a novel stable 1,3-dimetallic ITN derivative, monomer **1**, which can be used as a highly versatile building block for the construction of various ITN-containing conjugated polymers with different dihalogenated compounds through Stille-type reactions. We have shown the synthesis of three ITN-containing copolymers with alternating ITN−fluorene and ITN−thiophene structures, the properties of which, such as regioregularity, solubility, bandgap, and HOMO/LUMO levels, were controlled by the nature of the different comonomers. Our methodology thus provides new possibilities for the access of novel ITN-containing low bandgap polymers, the properties of which can be fine-tuned through careful design and selection of the dihalogenated coupling partners. The efficiencies of OPV devices using these ITN-containing copolymers are as high as 0.43%, and we are currently optimizing the reaction conditions toward polymer samples with higher molecular weights, testing various device fabrication strategies for better PV performances, and also pursuing new materials based on monomer **1**.[40]

Experimental Section

Materials and General Methods. Commercially available compounds were purchased from Aldrich and used as received. 3-Hexyl-2,5-diiodothiophene[34] and 2-bromo-3-decylthiophene[41] were synthesized according to literature procedures. Isothianaphthene was prepared according to the procedure described by Christensen et al.[30] and used immediately. THF and toluene were purified by first bubbling N_2 through for 30 min and then passing through a homemade column system.[42] Poly(3,4-ethylene dioxythiophene)/poly(styrenesulfonate) (PEDOT/PSS; Baytron P VP Al 4083) was provided from H.C. Starck. Methanofullerene [6,6]-phenyl C_{61}-butyric acid methyl ester (PCBM) was purchased from American Dye Sources (ADS). ITO glass slides (resistance 8−12 Ω/cm^2) were obtained from Delta Technologies. Heavily doped p-type Si wafers were provided from Silicon Valley Microelectronics. Air- and moisture-sensitive reactions were carried out under an atmosphere of prepurified nitrogen using either Schlenk techniques or an inert-atmosphere glovebox (MBraun). The 499.867 MHz ^{1}H NMR and 125.692 MHz ^{13}C NMR spectra were recorded on a Varian INOVA 500 MHz spectrometer. The 300.168 MHz ^{1}H NMR and 75.477 MHz ^{13}C NMR spectra were recorded on a Varian INOVA 300 MHz spectrometer. All solution ^{1}H and ^{13}C NMR spectra were referenced internally to the solvent peaks, and the labeling scheme is shown in Figure 2 and Figure S1. Elemental analysis was performed by Atlantic Microlab, Inc., Norcross, GA. Low-resolution mass spectra were obtained on a Finnigan MAT 95 mass spectrometer operating on EI (electron impact) mode. Samples were introduced by solid probe. Melting points were measured on a Perkin-Elmer Pyris Diamond TG/DTA 6300 instrument with ca. 5 mg sample at a heating rate of 10 °C/min. The results were reported from the apex of transition peak.

SEC analyses were performed in $CHCl_3$ (1 mL/min) using a Hewlett-Packard (HP) 1100 system equipped with a HP 1100 autosampler, a HP 1100 HPLC pump, a HP 1047A refractive index (RI) detector, and an Agilent 1200 UV−vis detector. Three styragel columns (Polymer Laboratories; 5 μm Mix-C), which were kept in a column heater at 35 °C, were used for separation. The columns were calibrated with polystyrene standards (Polymer Laboratories). Differential scanning calorimetry (DSC) measurements were acquired using a TA Q1000 calorimeter with ca. 10 mg of the polymer at a scan rate of 10 °C/min. The results reported are from the onset of the second heating cycle. An indium standard was used to calibrate the instrument, and nitrogen was used as the purge gas. Ultraviolet−visible (UV−vis) absorption spectra of polymer solutions and thin films were taken on a Spectronic Genesys 5 spectrometer over a wavelength range of 250−1100 nm. Solution measurements were performed in 1 cm quartz cuvettes, and polymer films were obtained by drop-casting *o*-dichlorobenzene solutions (ca. 5 mg/mL) onto ITO-coated glass substrates. Cyclic voltammetry was carried out on a 100B analyzer from BAS. The three-electrode system consisted of a glassy carbon disk as working electrode, a Ag wire as auxiliary electrode, and Ag/AgCl (calibrated with ferrocene$^{1+/0}$ couple, 0.40 V vs SCE in 0.1 M $[NBu_4][PF_6]$ acetonitrile solution[43]) as the reference electrode. Polymer films were obtained by drop-casting *o*-dichlorobenzene solutions (ca. 5 mg/mL) onto the glassy carbon electrode, and the cyclic voltammograms were recorded in CH_3CN containing $[Bu_4N][PF_6]$ (0.1 M) as the supporting electrolyte. The redox potentials are reported relative to the saturated calomel electrode (SCE). Matrix-assisted laser desorption/ionization−time-of-flight (MALDI-TOF) measurements were performed on the Bruker Reflex III instrument operating under linear mode. A typical sample was prepared by mixing 5 μL of a polymer solution in THF (5 mg/mL) and 15 μL of a dithranol solution in THF (20 mg/mL) and then spotting 1 μL of the mixture onto the sample plate. Cytochrome *c* (Bruker) were used externally for calibration. Film thickness was measured by a KLA Tencor P-16 profilometer. Wide-angle X-ray scattering (WAXS; Bruker-AXS microdiffractometer with 2.2 kW sealed Cu X-ray source) was performed to check the molecular packing status of drop-cast ITN-containing copolymers with thickness of ca. 4 μm. White Xe light (100 W, Oriel) that irradiated the OPV cell had an intensity of 100 mW/cm^2 (simulated AM 1.5 spectrum). Current−voltage characteristics of OPV cells were measured with a Keithley 2400 source meter controlled by customized LabView code. Photocurrent action spectra were obtained using a monochromator (Cornerstone 130 1/8 m) equipped with commercially available gratings and filters (Newport Corp.). Electrical characterization for the transistor was performed in the dark using a Desert Cryogenics probe station with a base pressure of 5×10^{-7} Torr. Mobility (μ) was calculated at the linear regime ($V_D = \pm 15$ V) using the equation $\mu = |\partial I_D/\partial V_G|_{V_D=\text{const}}/(C_i V_D W/L)$, where I_D, V_G, V_D, and C_i are drain current, gate voltage, drain voltage, and gate insulator SiO_2 capacitance (≈10 nF/cm^2).

PV Device Fabrication. PV devices were fabricated on precleaned patterned ITO glass substrates. PEDOT/PSS was spin-coated on the ITO glass slides (2.54 × 2.54 cm^2) at a speed of 4000 rpm for 45 s and annealed on 100−120 °C for 5 min. The PEDOT/PSS film was ca. 30 nm thick. On top of the PEDOT/PSS, a few drops of 1.7−3.7 wt % ITN-containing copolymer/PCBM in *o*-dichlorobenzene were deposited and then spin-coated at a speed of 600−800 rpm for 60 s inside a glovebox. The spun ITN-containing copolymer/PCBM films with various compositions were ca. 50−190 nm thick. After drying overnight by slow solvent evaporation, the spun film was mounted inside the bell jar of a Denton Vacuum Bench Top Turbo III thermal evaporator. Aluminum was evaporated to deposit a 100 nm thick electrode on top of the ITN-containing copolymer/PCBM films. The device active area was 9 mm^2.

Transistor Fabrication. Heavily doped p-type silicon wafers with 300 nm SiO_2 were used as the substrate for transistor fabrication. After removal of the SiO_2 from the backside, 10 nm Al and 75 nm Au were deposited by e-beam evaporation followed by rapid thermal annealing at 450 °C to form an ohmic contact. The SiO_2 side of the substrate was exposed to saturated hexamethyldisilazane (HMDS) vapor for several minutes. On top of the substrate, a few drops of 0.5 wt % polymer/fullerene solution (ITN-containing copolymer/PCBM in *o*-dichlorobenzene) were deposited and then spin-coated at a speed of 2000 rpm for 60 s in ambient laboratory conditions. The spun polymer/fullerene films were ca. 20 nm thick. Gold source and drain electrodes were formed via vacuum evaporation of 45 nm Au through a Si stencil mask. The transistor had a channel geometry of width ($W = 4000$ μm) and length ($L = 40$ μm).

Synthesis of 1,3-Di(trimethylstannyl)isothianaphthene (1). Freshly prepared isothianaphthene (4.36 g, 32.5 mmol) was dissolved in 100 mL of THF, and 12.2 mL of TMEDA (81.2 mmol) was added

through syringe. The mixture was cooled in an ice bath, and *n*-BuLi (2.5 M in hexanes) (31.2 mL, 78.0 mmol) was added dropwise through syringe. The ice bath was then removed, and the mixture was stirred at room temperature for 2 h before being cooled down to −78 °C. A chlorotrimethyltin solution (1.0 M in THF) (84 mL, 84 mmol) was then added dropwise through syringe. The mixture was slowly warmed up to room temperature and stirred overnight. The solution was poured into 200 mL of saturated NH_4HCO_3 and separated. The aqueous phase was extracted with ether twice, and the combined organic phase was washed with water three times and dried over $MgSO_4$. After removal of solvents under reduced pressure, **1** was isolated by recrystallization from petroleum ether as a pale yellow solid (9.3 g, 62%). ^{1}H NMR (499.867 MHz, C_6D_6): δ = 7.80 (dd, $^3J_{HH}$ = 6.5 Hz, $^4J_{HH}$ = 3.0 Hz, 2H, *H*4, 7), 7.07 (dd, $^3J_{HH}$ = 6.5 Hz, $^4J_{HH}$ = 3.0 Hz, 2H, *H*5, 6), 0.38 (s, 18H, Sn[CH_3]$_3$). ^{13}C NMR (75.477 MHz, C_6D_6): δ = 148.1 (*C*8, 9), 137.3 (*C*1, 3), 124.7 (*C*4, 7), 123.5 (*C*5, 6), −7.9 (Sn[CH_3]$_3$). Elemental analysis: calcd C 36.57, H 4.82, S 6.97%; found C 36.94, H 4.83, S 6.92%. Solid probe mass spectrometry (EI, 1500 Res.): calcd 459.8; found 460.0. Melting point: T_m = 104 °C.

Synthesis of 1,3-Di[2-(3-decylthienyl)]isothianaphthene (2). Monomer **1** (5.0 g, 10.9 mmol) and 2-bromo-3-decylthiophene (7.26 g, 23.9 mmol) were charged in a 50 mL Schlenk tube equipped with a magnetic stir bar under nitrogen, and 10 mL of toluene was added. After dissolution of the solid material, Pd[PPh_3]$_4$ (0.63 g, 0.55 mmol) in 10 mL of toluene was added, and the tube was left under partial vacuum and tightly sealed. The mixture was then immersed into an oil bath preset at 110 °C and stirred for 48 h; the completion of the reaction was signaled by precipitation of Pd black. All volatile materials were then removed under vacuum, and **2** was isolated as a yellow-greenish oil (4.68 g, 75%) by column chromatography on silica with petroleum ether as the eluent. ^{1}H NMR (300.168 MHz, $CDCl_3$): δ = 7.61 (dd, $^3J_{HH}$ = 6.6 Hz, $^4J_{HH}$ = 3.0 Hz, 2H, ITN-*H*4, 7), 7.39 (d, $^3J_{HH}$ = 5.4 Hz, 2H, Th-*H*5), 7.09 (m, 4H, ITN-*H*5, 6 and Th-*H*4), 2.67 (t, $^3J_{HH}$ = 7.5 Hz, 4H, CH_2[CH_2]$_8$$CH_3$), 1.60 (m, 4H, CH_2CH_2[CH_2]$_7$$CH_3$), 1.20 (br. 28H, CH_2CH_2[CH_2]$_7$$CH_3$), 0.87 (t, $^3J_{HH}$ = 6.8 Hz, 6H, CH_2CH_2[CH_2]$_7$CH_3).

Synthesis of 1,3-Di[2-(5-bromo-3-decylthienyl)]isothianaphthene (3). Compound **2** (3.74 g, 6.46 mmol) was dissolved in 100 mL of $CHCl_3$ and cooled in an ice bath. *N*-Bromosuccinimide (2.36 g, 13.2 mmol) was added in one portion in the dark. The ice bath was then removed, and the mixture was stirred in dark overnight. The organic phase was washed with saturated $NaHSO_3$ twice followed by saturated NaCl. Solvent was removed under reduced pressure, and the resultant orange oil was passed through a short silica column using petroleum ether as the eluent. Compound **3** was further purified by crystallization from acetone solution as a yellow solid (3.0 g, 63%). ^{1}H NMR (499.867 MHz, $CDCl_3$): δ = 7.58 (dd, $^3J_{HH}$ = 6.5 Hz, $^4J_{HH}$ = 3.0 Hz, 2H, ITN-*H*4, 7), 7.12 (dd, $^3J_{HH}$ = 7.0 Hz, $^4J_{HH}$ = 3.0 Hz, 2H, ITN-*H*5, 6), 7.04 (s, 2H, Th-*H*4), 2.59 (t, $^3J_{HH}$ = 8.0 Hz, 4H, CH_2[CH_2]$_8$$CH_3$), 1.56 (m, 4H, CH_2CH_2[CH_2]$_7$$CH_3$), 1.20 (br. 28H, CH_2CH_2[CH_2]$_7$$CH_3$), 0.87 (t, $^3J_{HH}$ = 7.5 Hz, 6H, CH_2CH_2[CH_2]$_7$CH_3). ^{13}C NMR (125.692 MHz, $CDCl_3$): δ = 143.5, 137.4, 132.3, 129.3, 125.4, 124.8, 121.4, 112.7 (aromatic ***C***'s), 32.1, 31.0, 29.8, 29.7, 29.5, 29.4, 29.2, 22.9, 14.3 (aliphatic ***C***'s). Melting point: T_m = 36 °C.

Synthesis of PITN-*co*-Fl. Monomer **1** (0.71 g, 1.54 mmol), 9,9′-dihexyl-2,7-dibromofluorene (0.76 g, 1.54 mmol), and tetrakis(triphenylphosphine)palladium(0) (0.178 g, 0.154 mmol) were dissolved in 10 mL of toluene and sealed in a reaction tube. The tube was immersed in an oil bath preset at 110 °C, and the mixture was stirred for 24 h. The completion of the reaction was indicated by precipitation of the catalyst as palladium black. The reaction mixture was then cooled down and filtered through a short plug of silica gel. **PITN-*co*-Fl** was isolated by repeated precipitation from $CHCl_3$ into acetone, dried under high vacuum at 60 °C for 12 h, and obtained as an orange powder (0.5 g, 70%). ^{1}H NMR (499.867 MHz, C_6D_6): δ = 8.2−7.0 (m, br aromatic *H*'s), 2.11, 1.98, 1.14, 0.81 (br aliphatic *H*'s). ^{13}C NMR (125.692 MHz, C_6D_6): δ = 152.9, 141.5, 136.6, 136.3, 134.6, 130.8, 125.2, 124.5, 121.4 (aromatic *C*'s), 56.3, 41.1, 40.7, 32.3, 32.1, 30.5, 24.8, 23.3, 14.7 (aliphatic *C*'s). SEC (RI): M_n = 3628, M_w = 19 919, PDI = 5.49. SEC (UV): M_n = 3751, M_w = 20 827, PDI = 5.55. DSC (onset, second heating curve): T_g = 27 °C. UV−vis (1.01×10^{-5} M in $CHCl_3$): λ_{max} = 339 nm, $\epsilon = 2.5 \times 10^4$ L mol^{-1} cm^{-1}, λ_{max} = 435 nm, $\epsilon = 2.3 \times 10^3$ L mol^{-1} cm^{-1}; UV−vis (film): λ_{max} = 339 nm.

Synthesis of PITN-*co*-3HT. Monomer **1** (2.18 g, 4.74 mmol), 3-hexyl-2,5-diiodothiophene (1.99 g, 4.74 mmol), and tetrakis(triphenylphosphine)palladium(0) (0.54 g, 0.474 mmol) were dissolved in 30 mL of toluene and sealed in a reaction tube. The tube was immersed in an oil bath preset at 90 °C, and the mixture was stirred for 72 h. The completion of the reaction was indicated by precipitation of the catalyst as palladium black. The reaction mixture was then cooled down and filtered through a short plug of silica gel. **PITN-*co*-3HT** was isolated by repeated precipitation from $CHCl_3$ into acetone, dried under high vacuum, and obtained as a black powder (0.4 g, 30%). ^{1}H NMR (499.867 MHz, C_6D_6): δ = 8.18, 7.88, 7.39, 6.97 (br aromatic *H*'s), 2.75, 1.62, 1.18, 0.84 (br aliphatic *H*'s). ^{13}C NMR (125.692 MHz, C_6D_6): δ = 144.5, 139.4, 138.5, 137.8, 136.7, 135.9 (aromatic *C*'s), 32.4, 32.3, 31.6, 31.1, 30.1, 29.8, 23.3, 14.7 (aliphatic *C*'s). SEC (RI): M_n = 5158, M_w = 9111, PDI = 1.51. SEC (UV): M_n = 4740, M_w = 10 057, PDI = 2.12. DSC (onset, second heating curve): T_g = 65 °C. UV−vis (2.24×10^{-5} M in $CHCl_3$): λ_{max} = 512 nm, $\epsilon = 9.6 \times 10^3$ L mol^{-1} cm^{-1}; UV−vis (film): λ_{max} = 533 nm.

Synthesis of PITN-*co*-3DT. Monomer **1** (0.384 g, 0.836 mmol), **3** (0.616 g, 0.836 mmol), and tetrakis(triphenylphosphine)palladium(0) (0.097 g, 0.084 mmol) were dissolved in 10 mL of toluene and sealed in a reaction tube. The tube was immersed in an oil bath preset at 110 °C, and the mixture was stirred for 24 h. The completion of the reaction was indicated by precipitation of the catalyst as palladium black. The reaction mixture was then cooled down and filtered through a short plug of silica gel. **PITN-*co*-3DT** was isolated by repeated precipitation from $CHCl_3$ into acetone, dried under high vacuum at 50 °C for 12 h, and obtained as a black powder (0.3 g, 51%). ^{1}H NMR (499.867 MHz, toluene-d_6): δ = 8.15, 7.90 (m, 4H, ITN-*H*4, 7), 7.41 (2H, Th-*H*), 7.02 (4H, ITN-*H*5, 6), 2.81 (4H, CH_2[CH_2]$_8$$CH_3$), 1.70 (4H, CH_2-CH_2[CH_2]$_7$$CH_3$), 1.31, 1.24 (28H, CH_2CH_2[CH_2]$_7$$CH_3$), 0.92 (6H, CH_2CH_2[CH_2]$_7$$CH_3$). ^{13}C NMR (125.692 MHz, toluene-d_6): δ = 143.9, 138.3, 137.6, 137.1, 136.5, 127.8, 126.9, 122.6 (aromatic C's), 32.8, 31.8, 30.6, 30.5, 30.4, 30.3, 30.2, 23.6, 14.8 (aliphatic C's). SEC (RI): M_n = 11 117, M_w = 27 543, PDI = 2.48. SEC (UV): M_n = 12 218, M_w = 33 941, PDI = 2.78. DSC (onset, second heating curve): T_g = 29 °C. UV−vis (1.68×10^{-5} M in $CHCl_3$): λ_{max} = 512 nm, $\epsilon = 8.1 \times 10^3$ L mol^{-1} cm^{-1}; UV−vis (film): λ_{max} = 546 nm.

Acknowledgment. The authors thank Dr. Dana Reed and Sean Murray for the help on the mass measurements and Prof. Kent R. Mann, Dr. Steve Drew, and Jonathan Bohnsack for the help on the cyclic voltammetry measurements. The Initiative for Renewable Energy and the Environment (IREE) at the University of Minnesota and the Xcel Energy Renewable Development Fund are gratefully acknowledged for financial support. J. Y. Kim thanks the Korea Research Foundation Grant funded by the Korean Government (MOEHRD) (KRF-2006-352-D00060).

Supporting Information Available: Synthetic details of 1,3-dipinacolborylisothianaphthene, NMR spectra of monomer **1**; mass spectrum of monomer **3**; SEC profiles, MALDI-TOF spectra, DSC plots, and cyclic voltammograms of the ITN-containing copolymers; charge mobility measurements using organic thin film transistor (OTFT) devices. This material is available free of charge via the Internet at http://pubs.acs.org.

References and Notes

(1) Roncali, J. *Chem. Rev.* **1997**, *97*, 173–205.
(2) Winder, C.; Sariciftci, N. S. *J. Mater. Chem.* **2004**, *14*, 1077–1086.

(3) Bundgaard, E.; Krebs, F. C. *Sol. Energy Mater. Sol. Cells* **2007**, *91*, 954–985.
(4) Scharber, M. C.; Mühlbacher, D.; Koppe, M.; Denk, P.; Waldauf, C.; Heeger, A. J.; Brabec, C. J. *Adv. Mater.* **2006**, *18*, 789–794.
(5) Shaheen, S. E.; Brabec, C. J.; Sariciftci, N. S.; Padinger, F.; Fromherz, T.; Hummelen, J. C. *Appl. Phys. Lett.* **2001**, *78*, 841–843.
(6) Coakley, K. M.; McGehee, M. D. *Chem. Mater.* **2004**, *16*, 4533–4542.
(7) Thompson, B. C.; Fréchet, J. M. J. *Angew. Chem., Int. Ed.* **2008**, *47*, 58–77.
(8) Brabec, C. J. *Sol. Energy Mater. Sol. Cells* **2004**, *83*, 273–292.
(9) Brabec, C. J.; Hauch, J. A.; Schilinsky, P.; Waldauf, C. *MRS Bull.* **2005**, *30*, 50–52.
(10) Wudl, F.; Kobayashi, M.; Heeger, A. J. *J. Org. Chem.* **1984**, *49*, 3382–3384.
(11) Colaneri, N.; Kobayashi, M.; Heeger, A. J.; Wudl, F. *Synth. Met.* **1986**, *14*, 45–52.
(12) Kobayashi, M.; Colaneri, N.; Boysel, M.; Wudl, F.; Heeger, A. J. *J. Chem. Phys.* **1985**, *82*, 5717–5723.
(13) Pomerantz, M.; Chaloner-Gill, B.; Harding, L. O.; Tseng, J. J.; Pomerantz, W. J. *Synth. Met.* **1993**, *55*−*57*, 960–965.
(14) King, G.; Higgins, S. J. *J. Mater. Chem.* **1995**, *5*, 447–455.
(15) Curran, S.; Roth, S.; Davey, A. P.; Drury, A.; Blau, W. *Synth. Met.* **1996**, *83*, 239–243.
(16) Ottenbourgs, B.; Paulussen, H.; Adriaensens, P.; Vanderzande, D.; Gelan, J. *Synth. Met.* **1997**, *89*, 95–102.
(17) Polec, I.; Henckens, A.; Goris, L.; Nicolas, M.; Loi, M. A.; Adreaensens, P. J.; Lutsen, L.; Manca, J. V.; Vanderzande, D.; Sariciftci, N. S. *J. Polym. Sci., Part A: Polym. Chem.* **2003**, *41*, 1034–1045.
(18) Goris, L.; Loi, M. A.; Cravino, A.; Neugebauer, H.; Sariciftci, N. S.; Polec, I.; Lutsen, L.; Andries, E.; Manca, J.; De Schepper, L.; Vanderzande, D. *Synth. Met.* **2003**, *138*, 249–253.
(19) Havinga, E. E.; ten Hoeve, W.; Wynberg, H. *Polym. Bull.* **1992**, *29*, 119–126.
(20) Havinga, E. E.; ten Hoeve, W.; Wynberg, H. *Synth. Met.* **1993**, *55*−*57*, 299–306.
(21) Bakhshi, A. K.; Bhargava, P. *J. Chem. Phys.* **2003**, *119*, 13159–13169.
(22) Mohanakrishnan, A. K.; Lakshmikantham, M. V.; McDougal, C.; Cava, M. P.; Baldwin, J. W.; Metzger, R. M. *J. Org. Chem.* **1998**, *63*, 3105–3112.
(23) Vangeneugden, D. L.; Kiebooms, R. H. L.; Vanderzande, D. J. M.; Gelan, J. M. J. V. *Synth. Met.* **1999**, *101*, 120–121.
(24) Shaheen, S. E.; Vangeneugden, D.; Kiebooms, R.; Vanderzande, D.; Fromherz, T.; Padinger, F.; Brabec, C. J.; Sariciftci, N. S. *Synth. Met.* **2001**, *121*, 1583–1584.
(25) Saito, H.; Ukai, S.; Iwatsuki, S.; Itoh, T.; Kubo, M. *Macromolecules* **1995**, *28*, 8363–8367.
(26) Itoh, Y.; Itoh, T.; Iwatsuki, S.; Kubo, M. *Polym. Bull.* **1996**, *37*, 155–160.
(27) Okuda, Y.; Lakshmikantham, M. V.; Cava, M. P. *J. Org. Chem.* **1991**, *56*, 6024–6026.
(28) Kiebooms, R. H. L.; Goto, H.; Akagi, K. *Macromolecules* **2001**, *34*, 7989–7998.
(29) 1,3-Dibromoisothianaphthene would be an alternative building block for conjugated polymers through Pd[0]-catalyzed coupling reactions. We attempted to make this compound through bromination of isothianaphthene using *N*-bromosuccinimide. That process led to only intractable black solid presumably due to oxidative polymerization. We did not pursue further in this direction for the following reasons: (i) The only example of this compound was described in a patent as a reaction intermediate (Itoh, K. U.S. Pat. Appl. Publ. US 2006057426, **2006**, 8 pp). The compound was not isolated or characterized. The stability of this compound is also questionable since the similar compound, 1,3-dichloroisothianaphthene, which is expected to be more stable, decomposes with time even at low temperature under an inert atmosphere (ref 27). (ii) It is generally accepted that in a Pd[0]-catalyzed coupling reaction the rate-limiting step is the oxidative insertion of aryl halide to the Pd species. The electron-rich isothianaphthene may thus slow down the insertion and destabilize the complex leading to side reactions and possible deactivation of the catalyst; see for example: Espinet, P.; Echavarren, A. M. *Angew. Chem., Int. Ed.* **2004**, *43*, 4704–4734.
(30) Christensen, P. A.; Kerr, J. C. H.; Higgins, S. J.; Hamnett, A. *Faraday Discuss. Chem. Soc.* **1989**, *88*, 261–275.
(31) Wudl et al. reported the preparation of a 1,3-dimercuryisothianaphthene derivative in 1978; see:Wudl, F.; Kruger, A. A.; Thomas, G. A. *Ann. N.Y. Acad. Sci.* **1978**, *313*, 79–85. 1,3-Dilithioisothianaphthene is another example of dimetallic ITN derivative that has not been isolated and thus could only be used as reaction intermediate.
(32) Stille, J. K. *Angew. Chem., Int. Ed.* **1986**, *25*, 508–524.
(33) Kosugi, M.; Fugami, K. *J. Organomet. Chem.* **2002**, *653*, 50–53.
(34) Mao, H.; Holdcroft, S. *Macromolecules* **1992**, *25*, 554–558.
(35) **PITN-*co*-3DT** was not soluble enough in C_6D_6 to obtain a well-resolved ^{13}C NMR spectrum, so instead toluene-d_8 was used. The polymer was completely dissolved in hot toluene-d_8 (∼15 mg/mL) and did not precipitate after the solution was cooled back down to room temperature.
(36) Brédas, J. L.; Silbey, R.; Boudreaux, D. S.; Chance, R. R. *J. Am. Chem. Soc.* **1983**, *105*, 6555–6559.
(37) Agrawal, A. K.; Jenekhe, S. A. *Chem. Mater.* **1996**, *8*, 579–589.
(38) van Duren, J. K. J.; Yang, X.; Loos, J.; Bulle-Lieuwma, C. W. T.; Sieval, A. B.; Hummelen, J. C.; Janssen, R. A. J. *Adv. Funct. Mater.* **2004**, *14*, 425–434.
(39) To further investigate the charge transport behavior of the PV devices, we measured the charge mobility of the polymer:PCBM (1:4 by weight) blends using gold bottom-gate and top-contact transistors setups (Figures S11 and S12). The electron mobility were recorded to be 2.4×10^{-4}, 3.3×10^{-4}, and 9.1×10^{-4} cm^2/(V s) for **PITN-*co*-Fl**, **PITN-*co*-3HT**, and **PITN-*co*-3DT**:PCBM blends, respectively. However, hole mobility could not be measured for these blend films. We also performed organic thin film transistor measurement on **PITN-*co*-3DT**, a relatively low hole mobility of 5.7×10^{-6} cm^2/(V s) was observed, presumably due to its amorphous nature.
(40) We are currently optimizing the reaction conditions and searching for other possible types of monomers and coupling reactions toward polymers with better properties, especially higher molecular weights. For example, a sample of **PITN-*co*-Fl** of higher molecular weight ($M_n = 7700$, $M_w = 13\,100$, PDI = 1.7) was obtained using Pd[P^{t}Bu$_3$]$_2$ (2 mol %) as the catalyst in THF at 80 °C for 24 h. We have also synthesized a 1,3-diborylated ITN derivative (B_2ITN) that shows much enhanced stability toward air and moisture; see Supporting Information for synthetic conditions and NMR characterization. We are currently investigating its polymerization with different dihalides through Suzuki-type coupling reactions.
(41) He, M.; Leslie, T. M.; Sinicropi, J. A. *Chem. Mater.* **2002**, *14*, 4662–4668.
(42) Pangborn, A. B.; Giardello, M. A.; Grubbs, R. H.; Rosen, R. K.; Timmers, F. J. *Organometallics* **1996**, *15*, 1518–1520.
(43) Connelly, N. G.; Geiger, W. E. *Chem. Rev.* **1996**, *96*, 877–910.

MA8011575